Radiation Physics and Chemistry 171 (2020) 108712

Contents lists available at ScienceDirect

Radiation Physics and Chemistry

journal homepage: www.elsevier.com/locate/radphyschem

Magnetic quenching of positronium studied by positron annihilation lifetime and Doppler broadening measurements

J.D. Liu[a], J.Q. Guo[a], M. Luo[a], Z. Wang[a], H.J. Zhang[a,*], B.J. Ye[a,**], Z.Q. Chen[b]

[a] State Key Laboratory of Particle Detection and Electronics, University of Science and Technology of China, Hefei 230026, China
[b] Hubei Nuclear Solid Physics Key Laboratory, Department of Physics, Wuhan University, Wuhan 430072, China

ARTICLE INFO

Keywords:
Positronium
Magnetic quenching
Positron annihilation lifetime
Doppler broadening

ABSTRACT

Annihilation of positronium (Ps) in static magnetic fields is investigated by positron annihilation lifetime (PAL) and Doppler broadening (DB) measurements of γ-Al_2O_3 nanopowder. The properties of four eigenstates of Ps atoms ($|1,1\rangle$, $|1,-1\rangle$, $|+\rangle$ (long-lived eigenstate mixed from $|1,0\rangle$ and $|0,0\rangle$ due to Zeeman effect), and $|-\rangle$ (short-lived eigenstate mixed from $|1,0\rangle$ and $|0,0\rangle$ due to Zeeman effect)) were revealed from PAL and DB results. Thereafter, with magnetic field increasing from 0.105 to 0.760 T, clear and regular variation of Ps annihilation parameters are observed: (1) The mean lifetime of the three long-lived Ps states ($|1,1\rangle$, $|1,-1\rangle$, and $|+\rangle$) shows clear quenching effect; (2) The formation probability of each Ps eigenstate ($|1,1\rangle$, $|1,-1\rangle$, $|+\rangle$, and $|-\rangle$) keeps unchanged; (3) The intensity of the narrow component (derived from multi-Gaussian fitting) of DB spectrum exhibits a gradual increase which is in good agreement with the theoretical calculation from PAL results (2γ decay of $|+\rangle$ and $|-\rangle$ states, and pick-off quenching of long-lived Ps states); (4) The intensity of the low energy region of DB spectrum is diminished by the decrease of 3γ decay of $|+\rangle$ state. The quantitative correlations between magnetic field and o-Ps annihilation parameters will be helpful for the further understanding of complex Ps quenching effects, such as the effect mixed from orhto-para spin conversion and magnetic quenching.

1. Introduction

Positronium (Ps), an exotic atom consisting of a positron (anti-particle of electron) and an electron, was theoretically predicted by Mohorovicic in 1934 and experimentally discovered by Deutsch in 1951 (Mohorovic, 1934; Deutsch, 1951). According to the spins of the positron and the electron, two types of Ps atoms exist: the spin-triplet ortho-positronium (o-Ps, $|S, m\rangle = |1,0\rangle, |1,1\rangle$, or $|1,-1\rangle$), and the spin-singlet para-positronium (p-Ps, $|S, m\rangle = |0,0\rangle$), where S and m are total spin and magnetic quantum number, respectively. The four eigenfunctions of Ps atoms are usually denoted as: $|1,1\rangle = \uparrow\Uparrow, |1,-1\rangle = \downarrow\Downarrow$, $|1,0\rangle = (\uparrow\Downarrow + \downarrow\Uparrow)/\sqrt{2}$, $|0,0\rangle = (\uparrow\Downarrow - \downarrow\Uparrow)/\sqrt{2}$, where ↑ and ⇑ correspond to electron and positron spin, respectively (Rich, 1981).

In vacuum, the ratio of p-Ps to o-Ps formation is 1 : 3, if positrons and electrons are not both spin-polarized. In vacuum and without an external magnetic field, p-Ps atoms mostly undergo self-annihilation by emitting two γ rays with the energy of ~ 511 keV, while the o-Ps atoms annihilate into three γ rays (to obey the charge-conjugation selection rule) with the energy ranging between 0 and 511 keV. The intrinsic self-annihilation lifetime of p-Ps and o-Ps, in vacuum and in the absence of magnetic field, is τ^{vac}_{p-Ps}=125.14 ps (the corresponding decay rate, inverse of lifetime, is $\lambda^{vac}_{p-Ps} = 7.9909 \times 10^9\ s^{-1}$) and τ^{vac}_{o-Ps}=142.04 ns ($\lambda^{vac}_{o-Ps} = 7.0401 \times 10^6\ s^{-1}$), respectively (Shibuya et al., 2013).

In conventional γ-Al_2O_3 powder, the lifetime of o-Ps is usually less than 20 ns and its intensity is usually less than 10% (Chen et al., 1995; Zhang et al., 2008). However, by using nanometer-sized γ-Al_2O_3 with a much higher specific surface area which is suitable for the efficient formation of Ps atoms, o-Ps lifetime largely increases to nearly 100 ns and the o-Ps intensity is greater than 20% (Paulin and Ambrosino, 1968; Brandt and Paulin, 1968; Trueba and Trasatti, 2005). Recently, our works on the formation and annihilation of Ps in several types of nanocomposites (prepared by loading the active components on the surfaces of porous γ-Al_2O_3 via impregnation method or solid reaction) have demonstrated that nanometer-sized γ-Al_2O_3 is quite suitable for Ps studies (Zhang et al., 2010, 2011, 2012; Liu et al., 2014).

Magnetic quenching of Ps atoms is a very interesting research topic in positron physics and atomic physics. Soon after the discovery of Ps, Deutsch studied the fine structure of Ps and measured the hyperfine splitting ΔW by using magnetic quenching (Deutsch and Dulit, 1951; Deutsch and Brown, 1952). In 1954, Halpern established the theory of

* Corresponding author.
** Corresponding author.
E-mail addresses: hjzhang8@ustc.edu.cn (H.J. Zhang), bjye@ustc.edu.cn (B.J. Ye).

https://doi.org/10.1016/j.radphyschem.2020.108712
Received 15 November 2019; Accepted 10 January 2020
Available online 17 January 2020
0969-806X/

magnetic quenching of Ps in static and alternating magnetic field by using perturbation approximation (Halpern, 1954). In 1962, Bisi et al. investigated magnetic quenching of Ps in teflon and lucite, and deduced the spin polarization of ~ 70% for ^{22}Na positron source (Bisi et al., 1962). In 1975, Mills Jr. developed the theory of magnetic quenching by using the matrices (Mills, 1975). In 1995, Nagashima et al. found Ps kinetic energy could only transfer to the translational motion of gas molecules, by measuring angular correlation of annihilation radiation (ACAR) spectra of SiO_2 powder, SiO_2 aerogel, and gas-filled SiO_2 aerogel in a magnetic field of 0.29 T (Nagashima et al., 1995). Most recently, Shibuya et al. studied the spin conversion and pick-off annihilation of o-Ps in gaseous Xe at elevated temperatures in a magnetic field of 0.832 T (Shibuya et al., 2013). Therefore from the quantitative study of magnetic quenching, we may obtain more detailed information of o-Ps and p-Ps to improve our understanding on Ps atoms.

To further understand Ps formation and annihilation, it will be helpful to study some mixed quenching effects of chemical quenching, spin conversion, and magnetic quenching etc. Therefore, in the present study we made an attempt to investigate magnetic quenching of Ps in γ-Al_2O_3 nanopowder in a series of static magnetic fields. Eventually, quantitative variations of various Ps eigenstates with increasing magnetic field were obtained.

2. Quenching of Ps

2.1. Quenching of Ps in the absence of magnetic field

Within a solid material, the relatively long lifetime enables o-Ps atoms to experience tremendous collisions with surrounding atoms prior to the final annihilation. In the absence of magnetic field, the lifetime of an o-Ps atom could be reduced drastically by emitting two γ rays of ~511 keV through the following four quenching mechanisms (Hyodo et al., 2009): ①pick-off quenching by picking up an electron with spin antiparallel to the positron in o-Ps atom (may shorten o-Ps lifetime to a wide range from a few ns to more than 100 ns, depending on the electron density of material surrounding o-Ps atoms); ②chemical quenching (such as iodine and CCl_4 (Tao, 1970; Chuang and Tao, 1970)); ③spin conversion quenching through electron exchange with unpaired electrons of paramagnetic atoms (such as gaseous O_2 (Shinohara et al., 2001), UV- and positron-irradiated SiO_2 aerogel and porous Al_2O_3 at low temperature (Saito and Hyodo, 1999), NiO (Zhang et al., 2010), and CoO (Liu et al., 2014)); ④spin conversion quenching through spin-orbit interaction with a heavy atom (such as gaseous Kr and Xe (Mitroy and Novikov, 2003; Saito and Hyodo, 2006; Shibuya et al., 2013)).

At a low temperature of several tens of kelvin, the UV- and positron-irradiated porous γ-Al_2O_3 could induce spin conversion of Ps through electron exchange with paramagnetic centers on the surfaces of Al_2O_3 grains (Saito and Hyodo, 1999). But at room temperature and in the absence of magnetic field, no other quenching effect was reported for γ-Al_2O_3 except pick-off quenching. In this study all positron measurements were performed at room temperature, therefore the decay rate of o-Ps in γ-Al_2O_3 could be expressed as: $\lambda_{o-Ps} = \lambda_{o-Ps}^{vac} + \lambda_{alumina}$, where $\lambda_{alumina}$ denotes the decay rate due to the pick-off quenching on the surfaces of γ-Al_2O_3 nanograins. The annihilation process of p-Ps atom is hardly influenced by γ-Al_2O_3 nanograins due to its extremely short lifetime. Thus in this study we could use the approximate relation: $\lambda_{p-Ps} \approx \lambda_{p-Ps}^{vac} = 7.9909 \times 10^9\ s^{-1}$.

2.2. Magnetic quenching of Ps

In the presence of magnetic field, two thirds of o-Ps atoms ($|1,1\rangle$ and $|1,-1\rangle$ states) keep their properties including lifetime and intensity. And one third of o-Ps atoms (in $|1,0\rangle$ state) mix with p-Ps ($|0,0\rangle$ state) atoms (namely Zeeman mixing) to form two new quantum states which could be denoted as $|+\rangle$ and $|-\rangle$. The four eigenstates of Ps atoms in a magnetic field could be expressed as (Rich, 1981; Shibuya et al., 2013):

$$|1,1\rangle, \tag{1}$$

$$|1,-1\rangle, \tag{2}$$

$$\left|+\right\rangle = \frac{1}{\sqrt{1+y^2}}\left|1,0\right\rangle - \frac{y}{\sqrt{1+y^2}}\left|0,0\right\rangle, \tag{3}$$

$$\left|-\right\rangle = \frac{y}{\sqrt{1+y^2}}\left|1,0\right\rangle + \frac{1}{\sqrt{1+y^2}}\left|0,0\right\rangle, \tag{4}$$

where $y = (\sqrt{1+x^2}-1)/x$ is derived from $x = 4\mu_0 B/\Delta W$, μ_0 is Bohr magneton, B is the magnetic field, and ΔW is the hyperfine splitting of Ps ground-state energy levels (0.842 meV, energy difference between the energy levels of ground-state o-Ps and p-Ps) (Consolati, 1996).

Under a static magnetic field, the decay rates of the four eigenstates are (Bisi et al., 1962):

$$\lambda_{|1,1\rangle} = \lambda_{o-Ps}, \tag{5}$$

$$\lambda_{|1,-1\rangle} = \lambda_{o-Ps}, \tag{6}$$

$$\lambda_{|+\rangle} = \frac{\lambda_{o-Ps} + y^2\lambda_{p-Ps}}{1+y^2}, \tag{7}$$

$$\lambda_{|-\rangle} = \frac{\lambda_{p-Ps} + y^2\lambda_{o-Ps}}{1+y^2}. \tag{8}$$

In a magnetic field of 1 T, the vacuum lifetime of $|+\rangle$ state is drastically quenched to 6.67 ns. But on the other hand, the vacuum lifetime of $|-\rangle$ state is only slightly increased to 127.42 ps. From the perspective of lifetime measurement, the significant shortening from 142.04 to 6.67 ns is observable and obvious, the slight increment from 125.14 to 127.42 ps is negligible and is below the detection limit of present PAL spectrometer. This is the reason why "Zeeman mixing" of Ps in a magnetic field was named as "magnetic quenching".

From Eq. (7) we can see that, the $|+\rangle$ state could decay into 3γ and 2γ rays. The ratio of 2γ to 3γ decays for the $|+\rangle$ state is (Rich, 1981):

$$r_{|+\rangle} = \frac{\lambda_{|+\rangle}^{2\gamma}}{\lambda_{|+\rangle}^{3\gamma}} = \frac{y^2\lambda_{p-Ps}}{\lambda_{o-Ps}}. \tag{9}$$

In the same sense, the ratio of 2γ to 3γ decays for the $|-\rangle$ state could be deduced from Eq. (8):

$$r_{|-\rangle} = \frac{\lambda_{|-\rangle}^{2\gamma}}{\lambda_{|-\rangle}^{3\gamma}} = \frac{\lambda_{p-Ps}}{y^2\lambda_{o-Ps}}. \tag{10}$$

3. Experiment

3.1. Samples and magnets

The γ-Al_2O_3 nanopowder (purity > 99.96%, grain size ~ 20 nm) was mixed with distilled water in an ultrasonic water bath at 80°C for 3 h. The mixture was dried overnight at 120°C and then calcined at 450°C for 10 h. The calcined compound was cooled down to the room temperature and hand-milled into powder. The milled powder was finally compressed into pellet-like (~ϕ15.0 × 2 mm) samples at a static pressure of 6 MPa for 5 min. Prior to PAL and DB measurements, γ-Al_2O_3 pellets were dried at 200°C for 2 h in air.

Each magnetic field applied to the samples was supplied by two identical cylinder-like permanent magnets ($Nb_2Fe_{14}B$, Aichi Steel Corp.). The distance between the two magnets was fixed to 4.5 mm. The strengths of the magnetic fields in the center of the space (ϕ20 × 4.5 mm) between two permanent magnets, which were adjusted by changing the magnets, were measured by a digital Gaussmeter (F. W. Bell Inc., Model 5080, accurate to 1%) before placing the sample-source-

sample sandwich between two permanent magnets. The strengths of magnetic fields measured by the Gaussmeter were: 0.105 T ($\phi 20 \times 1$), 0.158 T ($\phi 20 \times 1.5$), 0.195 T ($\phi 20 \times 2$), 0.285 T ($\phi 20 \times 3$), 0.362 T ($\phi 20 \times 4$), 0.420 T ($\phi 20 \times 5$), 0.660 T ($\phi 20 \times 10$), and 0.760 T ($\phi 20 \times 15$), where the numbers in the parentheses denote the size of the two identical magnets in mm for each magnetic field.

3.2. Positron measurements

The ^{22}Na positron source (~1×10^6 Bq) used in this study was produced by depositing and drying a droplet of ^{22}NaCl solution between two 10 × 10 × 0.02 mm Ti foils, where the ^{22}NaCl was confined to the central region ($\phi 2$ mm) of the two Ti foils. The ^{22}Na source was sandwiched between two γ-Al_2O_3 pellets by an Al foil with the thickness of 11 μm. The sample-source-sample sandwich (~$\phi 15 \times 4.5$ mm) and the two identical magnets were sealed in an Al pipe (outer diameter of 45 mm) which was evacuated by a turbo molecular pump backed by a scroll pump. The vacuum of the chamber is better than 1×10^{-5} Pa.

The PAL spectra were measured by a conventional fast-fast coincidence system with two scintillation (BaF_2 scintillator) detectors to collect the positron birth signals and the annihilation γ rays, respectively. To avoid magnetic disturbance to the photomultiplier tubes of PAL detectors, the two PAL detectors were shielded by two μ-metal (alloy notable for high magnetic permeability, composed of 77% Ni, 16% Fe, 5% Cu, and 2% Mo) tubes. The energy window of the start discriminator was adjusted to collect the birth signals (γ ray of 1.274 MeV) of the positrons from the ^{22}Na source. The lower level of the energy window of stop discriminator was fixed to the minimum to record the γ rays including the 3γ decay of o-Ps atoms (energy ranging from 0 to 511 keV). The time range of time-to-amplitude converter (TAC) was set to 200 ns. The total channel number is 4096, and the time scale is 50.0 ps/channel. The time resolution of PAL spectrometer is ~ 270 ps. The two PAL detectors were positioned close to the Al pipe, and the resulted counting rate was ~ 380 counts per second (cps). Each PAL spectrum was collected to a total count of ~4×10^6.

The DB spectra were measured by a HP-Ge detectors (ORTEC, GEM−10185−P model) with the energy resolution (FWHM) of 1.39 keV at 511 keV (1.85 keV at 1.33 MeV). The distance between the DB detector and the sample was ~ 28 cm. The total channel number of analog-to-digital convertor (ADC) is 8192, and the channel width of ADC is 85.57 eV/channel (calibrated by Eu-152 isotope). The center of 511 keV peak was set to 6000 channel prior to the DB experiments, and the peak shift is no more than 2 channels during the DB measurements. The total count of each DB spectrum is more than 6×10^6, and the counting rate is around 680 cps.

4. Results and discussion

4.1. The lifetimes of the long-lived Ps states

In conventional lifetime analysis, a PAL spectrum (the variation of positron annihilation events as a function of the time) is a sum of several negative exponentials (Schrader and Jean, 1988; Deng and Jean, 1993):

$$y(t) = R(t)*\left(N(t)\sum_{i=1}^{n}\frac{I_i}{\tau_i}e^{-t/\tau_i} + B_g\right) \quad (11)$$

where $R(t)$ is instrument resolution function, the asterisk denotes for a convolution, $N(t)$ is the total number of annihilation events, τ_i is the lifetime of the i-th component, I_i is the intensity of the i-th component, and B_g is the background.

In porous materials, the PAL spectra are usually resolved into four or five lifetime components due to the wide volume distribution of free volumes. In this study, all PAL spectra were resolved into four lifetime components by using PATFIT program (Kirkegaard et al., 1989). Due to the long tail formed by o-Ps annihilation, the average count before lifetime peak was selected as the background of each PAL spectrum. The lifetime components of o-Ps atoms ($\tau > 1$ ns) correspond to different sizes of free volumes in the sample (Tao, 1972; Ito et al., 1999; Lue et al., 2008). In the pellets compressed from γ-Al_2O_3 nanopowder, the free volume (the free space between the γ-Al_2O_3 nanograins) has a very wide volume distribution. So the lifetime component of o-Ps resolved from PATFIT software is the statistical average of the free volumes between the nanograins.

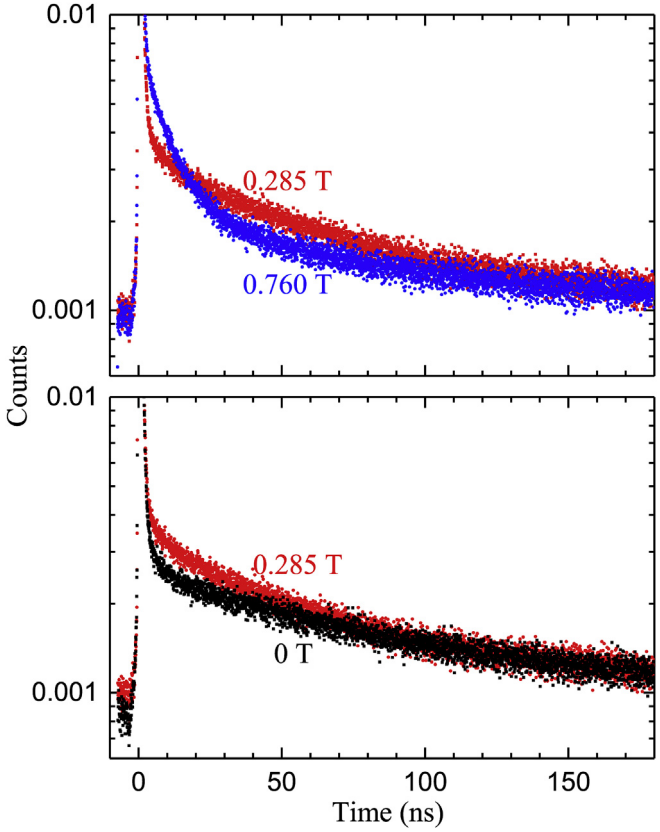

Fig. 1. The PAL spectra of γ-Al_2O_3 in a magnetic field of 0, 0.285, and 0.760 T. The count of the lifetime peak (0 ns) was normalized to 1 for each spectrum. To observe the tails of lifetime spectra, upper regions of the peaks (the counts between 0.01 and 1) are not shown. (For interpretation of the references to colour in this figure legend, the reader is referred to the Web version of this article.)

The PAL spectra of γ-Al_2O_3 in a magnetic field of 0, 0.285, and 0.760 T are shown in Fig. 1. The long lifetime tail (in the time range between ~ 50 and 180 ns) of PAL spectrum measured at 0 T, which could not be well fitted by a straight line, shows the wide volume distribution of the free volumes in γ-Al_2O_3 sample. In a magnetic field of 0.285 T, the slope of the long lifetime tail shows a tiny increase to the case of no magnetic field. This implies the shortening of the longest lifetime component in a magnetic field. While in a magnetic field of 0.760 T, the slope of the long lifetime tail decreases significantly than at 0.285 T, which means the longest lifetime component measured at 0.760 T is longer than that at 0.285 T.

In the absence of magnetic field, two short (shorter than 1 ns) and two long lifetime components (longer than 1 ns) were resolved from PAL spectrum of γ-Al_2O_3 pellets. The lifetime component τ_3 of 2.74±0.09 ns (intensity of $I_3 = (1.69 \pm 0.04)\%$) is attributed to the pick-off quenching of o-Ps in some microvoids inside of γ-Al_2O_3 nanograins. The longest lifetime component τ_4 of 101.10±0.49 ns (intensity of $I_4 = (23.95 \pm 0.05)\%$) corresponds to the annihilation of o-Ps in the free volumes between γ-Al_2O_3 nanograins. So in the absence of magnetic field, the total intensity of o-Ps atoms in γ-Al_2O_3 pellets is

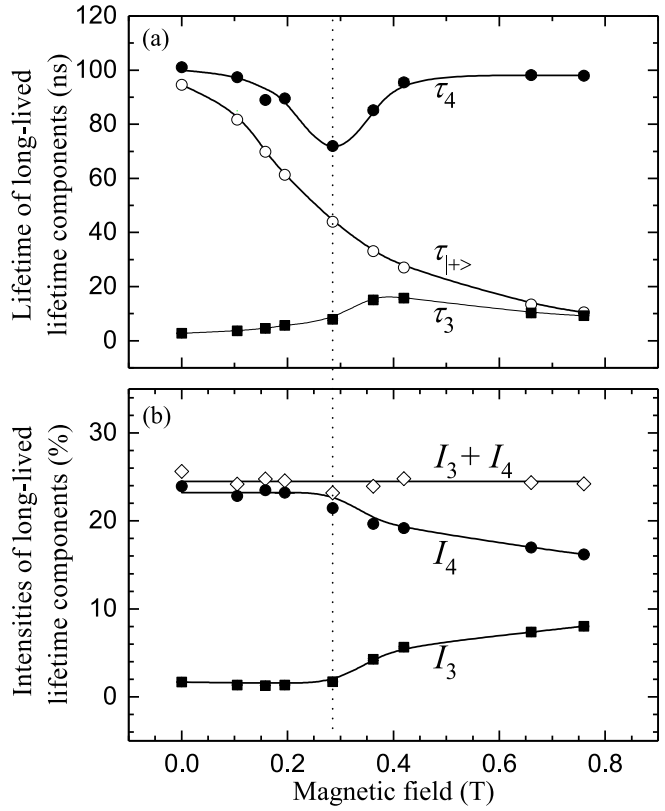

Fig. 2. (a) Variation of long-lived lifetime components τ_4 and τ_3 as a function of magnetic field. The lifetimes of $|+\rangle$ state ($\tau_{|+\rangle}$) derived from magnetic quenching theory are plotted to compare with τ_4 and τ_3. (b) Variation of intensities of long-lived lifetimes I_4, I_3, and their sum $I_3 + I_4$ as a function of magnetic field.

$I_{o-Ps} = I_3 + I_4 = 25.64\%$, the average lifetime of o-Ps atoms is $\tau_{o-Ps} = (I_3\tau_3 + I_4\tau_4)/(I_3 + I_4) = 94.61$ ns, and the corresponding decay rate is $\lambda_{o-Ps} = 1/\tau_{o-Ps} = 1.0570 \times 10^7\ s^{-1}$.

As shown in Fig. 2, the variation of τ_3, τ_4, I_3, and I_4 as a function of magnetic field could be approximately divided into two stages with the magnetic field lower or higher than 0.285 T. In the first stage with magnetic field increasing up to 0.285 T, τ_4 decreases obviously from ~ 100 to ~ 70 ns, while τ_3 shows only a very small increment, but I_4 and I_3 nearly keep unchanged. In the second stage with magnetic field increasing from 0.285 to 0.760 T, τ_4 first increases back to ~ 100 ns and then keeps it as a constant, τ_3 first increases abruptly and then decreases gradually, I_4 decreases while I_3 increases.

The lifetime of $|+\rangle$ state could be derived from Eq. (7) as:

$$\tau_{|+\rangle} = \lambda_{|+\rangle}^{-1} = \left(\frac{\lambda_{o-Ps} + y^2\lambda_{p-Ps}}{1+y^2}\right)^{-1}. \tag{12}$$

The variation of $\tau_{|+\rangle}$, which is calculated with λ_{o-Ps} of $1.0570 \times 10^7\ s^{-1}$ and λ_{p-Ps} of $7.9909\times 10^9\ s^{-1}$, is also plotted in Fig. 2(a). By comparing the tendency of $\tau_{|+>}$ to those of τ_3 and τ_4, the variation of I_3 and I_4 could be interpreted naturally: (1) in the first stage, $\tau_{|+\rangle}$ is close to $\tau_{|1,\pm1\rangle}$ (difficult to tell $\tau_{|+>}$ from $\tau_{|1,\pm1\rangle}$ due to the wide volume distribution of free volumes in γ-Al_2O_3 nanopowder), thus induces obvious decrease of τ_4 but no apparent decrease of I_4; (2) in the second stage, $\tau_{|+\rangle}$ tends to be much smaller than $\tau_{|1,\pm1\rangle}$ (quite easy to be distinguished from $\tau_{|1,\pm1\rangle}$), therefore induces significant decrease of I_4 and increase of I_3.

As shown in Fig. 2(b), the sum of I_3 and I_4, which equals to the total intensity of the three long-lived Ps states, is independent of magnetic field:

$$I_{|1,1\rangle} + I_{|1,-1\rangle} + I_{|+\rangle} = I_3 + I_4 = 25.64\%. \tag{13}$$

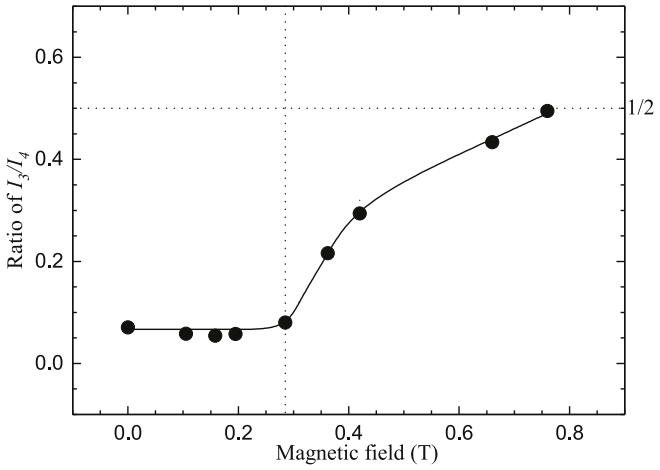

Fig. 3. Variation of I_3/I_4 as a function of magnetic field.

To investigate the variation of I_3 and I_4 with increasing magnetic field more carefully, I_3/I_4 is plotted in Fig. 3. For the case of no magnetic field, I_3/I_4 of 0.07 is the ratio of o-Ps atoms annihilate in microvoids (inside the nanograins) and free volumes (between the nanograins). The variation of I_3/I_4 ratio also behaves differently in the two stages. In the first stage, the I_3/I_4 nearly keeps as a constant at 0.07. This means, in a weak magnetic field, the lifetime difference between $|+\rangle$ and $|1, \pm1\rangle$ is small, τ_4 is the mean lifetime of the three long-lived o-Ps atoms ($|1,1\rangle$, $|1,-1\rangle$, and $|+\rangle$ states), so I_4 and I_3 reflect similar information with that in the absence of magnetic field. But in the second stage, I_3/I_4 quickly increases and finally reaches to a value of 0.50 at 0.760 T. The increase of I_3/I_4 implies that, in a strong magnetic field, with decreasing lifetime of $|+\rangle$ state, I_3 tends to include the annihilation of $|+\rangle$ in free volumes besides the long-lived Ps atoms in microvoids. At the magnetic field of 0.760 T, nearly all the annihilation of $|+\rangle$ state was distinguished from that of $|1, \pm1\rangle$ states. Thereafter $I_3/I_4 = 0.50$ at 0.760 T implies that:

$$I_{|+\rangle} = \frac{I_{|1,1\rangle} + I_{|1,-1\rangle}}{2}. \tag{14}$$

Because the $|+\rangle$ and $|-\rangle$ states are mixed from $|1,0\rangle$ and $|0,0\rangle$ by Zeeman effect, we have:

$$I_{|+\rangle} + I_{|-\rangle} = I_{|1,0\rangle} + I_{|0,0\rangle}. \tag{15}$$

Considering the formation probabilities of $|1,1\rangle$ and $|1, -1\rangle$ are not affected by magnetic field,

$$I_{|1,1\rangle} = I_{|1,-1\rangle}. \tag{16}$$

Finally, from the above four equations, we could have a simple result:

$$I_{|1,1\rangle} = I_{|1,-1\rangle} = I_{|+\rangle} = I_{|-\rangle} = \frac{I_3 + I_4}{3} = 8.55\%. \tag{17}$$

This clarifies the formation probability of each Ps state is not affected by magnetic field.

From the analysis of Figs. 2 and 3, we understand that the lifetime of $\tau_{|+\rangle}$ in porous materials is difficult to be extracted from PAL spectra especially in a weak magnetic field. To compare our experimental results with the theoretical prediction, it is necessary to compare the average of three long-lived lifetimes of $\tau_{|1,1\rangle}$, $\tau_{|1,-1\rangle}$, and $\tau_{|+\rangle}$. The mean lifetime of the three long-lived states derived from magnetic quenching theory, $\overline{\tau_{long}^{theo}}$, could be written in (Rochanakij and Schrader, 1988):

$$\overline{\tau_{long}^{theo}} = \frac{\tau_{|1,1\rangle}}{3} + \frac{\tau_{|1,-1\rangle}}{3} + \frac{\tau_{|+\rangle}}{3} = \frac{2}{3}\tau_{o-Ps} + \frac{1}{3}\tau_{|+\rangle}. \tag{18}$$

From the resolved long-lived lifetime components of PAL spectra, the mean lifetime of the two long-lived lifetime components could be calculated from:

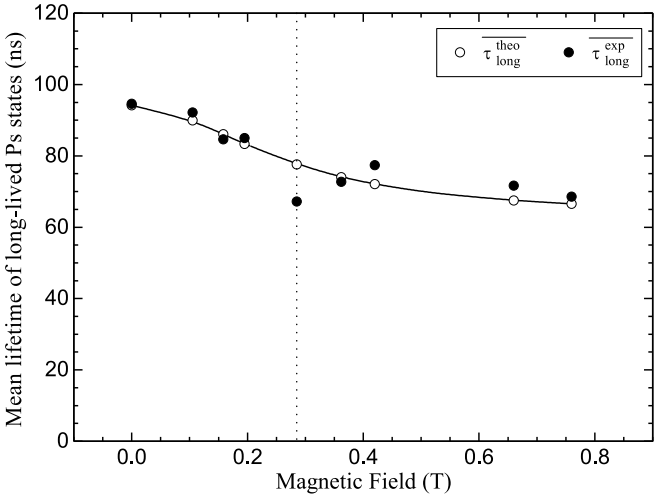

Fig. 4. Mean lifetime of the three long-lived Ps states (|1,1⟩, |1, −1⟩, and |+⟩) as a function of magnetic field. The open circles and the filled circles denote the values of $\overline{\tau}^{\text{theo}}_{\text{long}}$ (deduced from magnetic quenching theory) and $\overline{\tau}^{\text{exp}}_{\text{long}}$ (mean lifetime of the two long lifetime components τ_3 and τ_4 of experimental PAL spectra), respectively.

$$\overline{\tau}^{\text{exp}}_{\text{long}} = \frac{I_3\tau_3 + I_4\tau_4}{I_3 + I_4}. \tag{19}$$

As shown in Fig. 4, $\overline{\tau}^{\text{exp}}_{\text{long}}$ from the PAL spectra (shown as filled circles), are in good agreement with $\overline{\tau}^{\text{theo}}_{\text{long}}$ obtained from magnetic quenching theory (shown as open circles).

4.2. Intensities of the narrow components of DB spectra

The 511 keV peak of each Doppler broadening (DB) spectrum was decomposed into three components by multi-Gaussian fitting (Skalsey et al., 1998; Chen et al., 2004, 2005; Sato et al., 2005; Zhang et al., 2010, 2012). Among the three components, the narrow component (its FWHM is usually less than 1.5 keV) corresponds to the 2γ decay of p-Ps atoms. The feasibility of the multi-Gaussian fitting is attributed to the nearly zero momenta of p-Ps atoms.

In solid materials and in the absence of magnetic field, the formation ratio of p-Ps to o-Ps is 1 : 3, if the positrons and electrons are not both spin-polarized. The ratio between I^{nr} (intensity of the narrow component of DB spectrum) and $I_{\text{o-Ps}}$ (o-Ps intensity resolved from PAL spectrum) is usually larger than 1 : 3 due to the pick-off quenching of o-Ps atoms into 2 γ rays. From the multi-Gaussian fitting of DB spectrum in the absence of magnetic field, the narrow component has a FWHM of 1.48 keV and an intensity of 9.98%.

The pick-off quenching of long-lived Ps states, which finally decays into 2 γ rays, is due to the tremendous collisions of long-lived Ps atoms with the walls of free volumes. In the absence of magnetic field, the intensity of the narrow component decomposed from DB spectrum may be written as:

$$I^{\text{nr}} = I_{\text{p-Ps}} + I^{2\gamma}_{\text{pick-off}} = I_{\text{p-Ps}} + R^{2\gamma}_{\text{pick-off}} I_{\text{o-Ps}}, \tag{20}$$

where $I^{2\gamma}_{\text{pick-off}}$ is the increment of I^{nr} induced by pick-off quenching into 2 γ rays, $R^{2\gamma}_{\text{pick-off}}$ is the fraction of long-lived Ps atoms which experience pick-off quenching into 2 γ rays and result in the increase of I^{nr}. So from $I^{\text{nr}}/I_{\text{o-Ps}} = 9.98\%/(1.69\ \% + 23.95\%) = 38.91\%$, we could have a $R^{\text{nr}}_{\text{pick-off}}$ value of 5.58% for the γ-Al_2O_3 samples.

In a magnetic field, the intensity of the narrow component of DB spectrum (I^{nr}) of γ-Al_2O_3 comprises three parts contributed from: 2γ decay of |+⟩; 2γ decay of |−⟩; and pick-off quenching of long-lived Ps atoms (|1,1⟩, |1, −1⟩, and 3γ decay fraction of |+⟩ state). Thereafter, the total intensity of the narrow component of DB spectrum derived from magnetic quenching theory, is the sum of the above three parts:

$$I^{\text{nr}}_{\text{theo}} = I^{2\gamma}_{|+\rangle} + I^{2\gamma}_{|-\rangle} + I^{2\gamma}_{\text{pick-off}} \tag{21}$$

Based on magnetic quenching theory, the intensity of the narrow component (I^{nr}) contributed by 2γ decay of |+⟩ state could be derived from Eq. (9):

$$I^{2\gamma}_{|+\rangle} = \frac{r_{|+\rangle}}{1 + r_{|+\rangle}} I_{|+\rangle} = \frac{y^2\lambda_{\text{p-Ps}}}{\lambda_{\text{o-Ps}} + y^2\lambda_{\text{p-Ps}}} I_{|+\rangle} \tag{22}$$

In the same sense, the intensity of the narrow component contributed by 2γ decay of |−⟩ state derived from Eq. (10) is:

$$I^{2\gamma}_{|-\rangle} = \frac{r_{|-\rangle}}{1 + r_{|-\rangle}} I_{|-\rangle} = \frac{\lambda_{\text{p-Ps}}}{\lambda_{\text{p-Ps}} + y^2\lambda_{\text{o-Ps}}} I_{|-\rangle} \tag{23}$$

The probability of pick-off quenching is proportional to the lifetime of the long-lived Ps atoms (i.e. the number of the collisions with the walls of free volumes before the final annihilation). The |1,1⟩ and |1, −1⟩ states keep their original lifetime in a magnetic field, so their pick-off quenching to induce 2γ decay ($R^{2\gamma}_{\text{pick-off}}$) must not change. While for 3γ decay fraction of |+⟩ state (its intensity is $I_{|+\rangle} - I^{2\gamma}_{|+\rangle}$), the increment of $I^{2\gamma}_{\text{pick-off}}$ induced by pick-off quenching must be lower than that of |1, ±1⟩ states due to its shorter lifetime (i.e. less collisions before annihilation). From this point of view, the intensity of the narrow component of DB spectrum in a magnetic field induced by the pick-off quenching effect should be expressed as:

$$\begin{aligned} I^{2\gamma}_{\text{pick-off}} &= R^{2\gamma}_{\text{pick-off}}\left(I_{|1,1\rangle} + I_{|1,-1\rangle} + \frac{\tau_{|+\rangle}}{\tau_{\text{o-Ps}}} I^{3\gamma}_{|+\rangle}\right) \\ &= R^{2\gamma}_{\text{pick-off}}\left[I_{|1,1\rangle} + I_{|1,-1\rangle} + \frac{\tau_{|+\rangle}}{\tau_{\text{o-Ps}}}\left(I_{|+\rangle} - I^{2\gamma}_{|+\rangle}\right)\right]. \end{aligned} \tag{24}$$

The variation of $I^{2\gamma}_{|+\rangle}$, $I^{2\gamma}_{|-\rangle}$, $I^{2\gamma}_{\text{pick-off}}$, and $I^{2\gamma}_{\text{theo}}$ with increasing magnetic field are plotted in Fig. 5. With magnetic field increasing from 0 to 0.760 T, the tendencies of the four intensities of the narrow component derived from the magnetic quenching are obvious: (a) $I^{2\gamma}_{|+\rangle}$ drastically increases from 0 to 7.61% ($r_{|+\rangle} = \lambda^{2\gamma}_{|+\rangle}/\lambda^{3\gamma}_{|+\rangle} = y^2\lambda_{\text{p-Ps}}/\lambda_{\text{o-Ps}} = 8.08$ for 0.760 T), (b) $I^{2\gamma}_{|-\rangle}$ nearly keeps as a constant at 8.55% ($r_{|-\rangle} = \lambda^{2\gamma}_{|-\rangle}/\lambda^{3\gamma}_{|-\rangle} = \lambda_{\text{p-Ps}}/(y^2\lambda_{\text{o-Ps}}) \approx 70743$ for 0.760 T), (c) $I^{2\gamma}_{\text{pick-off}}$ decreases slightly from 1.43% to 0.96% (for 0.760 T, $\tau_{|+\rangle}/\tau_{\text{o-Ps}} = 11.13\%$, and $I_{|+\rangle} - I^{2\gamma}_{|+\rangle} = 0.94\%$), (d) $I^{2\gamma}_{\text{theo}}$ shows similar variation tendency with that of $I^{2\gamma}_{|+\rangle}$ (the changes of $I^{2\gamma}_{\text{pick-off}}$ and $I^{2\gamma}_{|-\rangle}$ are negligible comparing to that of $I^{2\gamma}_{|+\rangle}$).

The total intensity of the narrow component of DB spectrum in a magnetic field derived from magnetic quenching theory ($I^{\text{nr}}_{\text{theo}}$) could be compared with that from multi-Gaussian fitting of experimental DB spectrum ($I^{\text{nr}}_{\text{exp}}$). From Fig. 5 we could see clearly that, the experimental DB results $I^{\text{nr}}_{\text{exp}}$ (plotted as filled circles) are in good agreement with $I^{\text{nr}}_{\text{theo}}$ (shown as open circles). The consistence of $I^{\text{nr}}_{\text{exp}}$ and $I^{\text{nr}}_{\text{theo}}$ strongly proved the correctness of magnetic quenching theory and the reliability of multi-Gaussian fitting to analyze 2γ decay of Ps atoms.

4.3. The FWHM of the narrow components of DB spectra

The raw and deconvoluted peaks of the DB spectra measured at 0, 0.105, 0.285, and 0.760 T are shown in Fig. 6. We can see clear narrowing of the 511 keV peak with increasing magnetic field, which is consistent with the previous reports (Itoh et al., 1993; Nagashima et al., 1995). The FWHM of the narrow component was also obtained in the data processing of multi-Gaussian fitting of DB spectrum. As shown in Fig. 7, the FWHM first quickly drops from 1.48 to 1.39 keV at 0.285 T, and then slowly decreases and finally saturates to 1.37 keV. As shown in Fig. 5, the increment of intensity of the narrow component in a magnetic field is mainly determined by 2γ decay of |+⟩ state. This could be proved by similar shape of the variation curves of the FWHM of the narrow component (shown as blue circles) and $I^{2\gamma}_{|+\rangle}$ (shown as red asterisks).

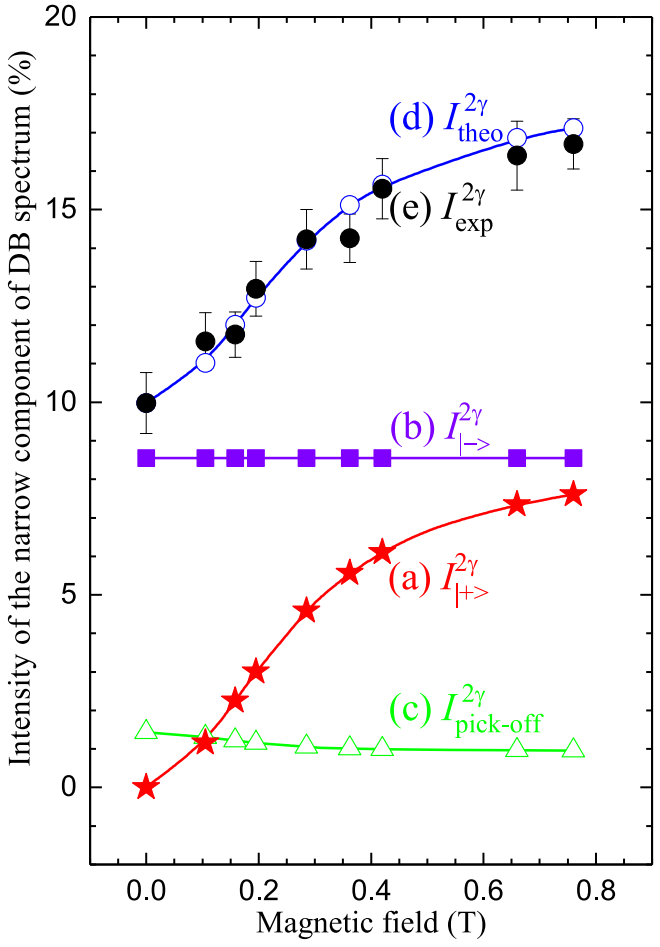

Fig. 5. Intensity of the narrow component of DB spectrum as a function of magnetic field for (a) $I^{2\gamma}_{|+\rangle}$ (from 2γ decay of $|+\rangle$ state), (b) $I^{2\gamma}_{|-\rangle}$ (from 2γ decay of $|-\rangle$ state), (c) $I^{2\gamma}_{pick-off}$ (from pick-off quenching of $|1,1\rangle$, $|1,-1\rangle$, and $|+\rangle$ states), (d) $I^{2\gamma}_{theo}$ (the sum of (a), (b), and (c), derived from magnetic quenching theory), (e) I^{nr}_{exp} (the narrow component resolved from experimental DB spectrum by multi-Gaussian fitting). (For interpretation of the references to colour in this figure legend, the reader is referred to the Web version of this article.)

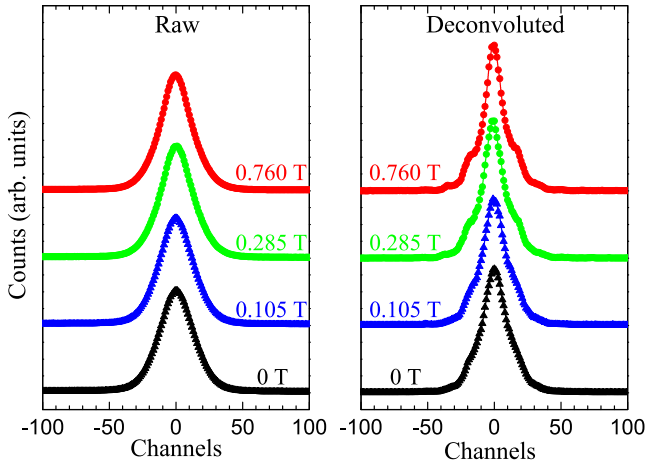

Fig. 6. The raw and deconvoluted peaks of the DB spectra in a magnetic field of 0, 0.105, 0.285, and 0.760 T. The center of the peak was normalized to 0 channel for each spectrum. (For interpretation of the references to colour in this figure legend, the reader is referred to the Web version of this article.)

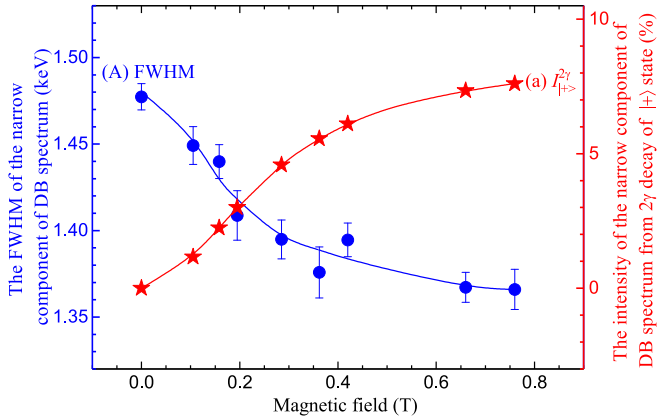

Fig. 7. Variation of (A) the FWHM of the narrow component of DB spectrum, (a) $I^{2\gamma}_{|+\rangle}$ (intensity of the narrow component of DB spectrum contributed from 2γ decay of $|+\rangle$ state) as a function of magnetic field. (For interpretation of the references to colour in this figure legend, the reader is referred to the Web version of this article.)

In the absence of magnetic field, the narrow component of DB spectrum is contributed by self-annihilation of p-Ps and pick-off quenching of o-Ps. Narrowing of 511 keV peak in a magnetic field due to 2γ decay of $|+\rangle$ state clarifies that, the momentum of Ps atom in $|+\rangle$ state is smaller than that in $|-\rangle$ state. The Ps atom in $|+\rangle$ state has a lifetime much longer than that in $|-\rangle$ state ($\tau_{|+\rangle}/\tau_{|-\rangle}$ = 10.53 ns/126.48 ps = 83.25 at 0.760 T), therefore it must experience much more collisions to reach a momentum much lower than that of $|-\rangle$ state. This is consistent with our previous report that the narrowing of the narrow component of DB spectrum while the spin conversion of o-Ps atoms appears. The p-Ps atom converted from o-Ps (spin conversion of o-Ps through electron exchange with paramagnetic NiO atoms) has a momentum lower than that of as-formed p-Ps due to the longer lifetime (i. e. more collisions) (Zhang et al., 2010, 2012).

4.4. The low energy region of DB spectra

Besides characterizing 2γ decay of Ps atoms via multi-Gaussian fitting of 511 keV peak of a DB spectrum, we could reveal the information of 3γ decay of Ps atoms via investigating the low energy region before 511 keV peak. The emitted three γ rays has a wide energy distribution between 0 and 511 keV and nearly has no contribution to the 511 keV peak of DB spectrum (Coleman, 2000).

In Fig. 8 we show the DB spectra of γ-Al_2O_3 measured in a magnetic field of 0, 0.105, 0.285, and 0.760 T. To observe the tiny change in the low energy region before 511 keV peak, the upper part (from 2×10^4 to 1×10^5 counts) of each 511 keV peak (near 6000 channel) is not shown. It is apparent that the intensity of the low energy region decreased with increasing magnetic field. This indicates that the 3γ decay of Ps is suppressed by magnetic field.

From magnetic quenching theory, the intensity of 3γ decay of Ps atoms ($I^{3\gamma}_{Ps}$), which is contributed from 3γ decay of all four states, could be written as:

$$I^{3\gamma}_{Ps} = I^{3\gamma}_{|1,1\rangle} + I^{3\gamma}_{|1,-1\rangle} + I^{3\gamma}_{|+\rangle} + I^{3\gamma}_{|-\rangle}, \quad (25)$$

where $I^{3\gamma}_{|1,1\rangle}$, $I^{3\gamma}_{|1,-1\rangle}$, $I^{3\gamma}_{|+\rangle}$, and $I^{3\gamma}_{|-\rangle}$ correspond to the intensities of 3γ decay for $|1,1\rangle$, $|1,-1\rangle$, $|+\rangle$, and $|-\rangle$, respectively. Considering the diminution of 3γ decay of long-lived Ps states by pick-off quenching of $I^{3\gamma}_{|1,1\rangle}$, $I^{3\gamma}_{|1,-1\rangle}$, and $I^{3\gamma}_{|+\rangle}$, the intensities of 3γ decay for the four Ps states could be expressed as:

$$I^{3\gamma}_{|1,1\rangle} = (1 - R^{2\gamma}_{pick-off}) I_{|1,1\rangle}, \quad (26)$$

$$I^{3\gamma}_{|1,-1\rangle} = (1 - R^{2\gamma}_{pick-off}) I_{|1,-1\rangle}, \quad (27)$$

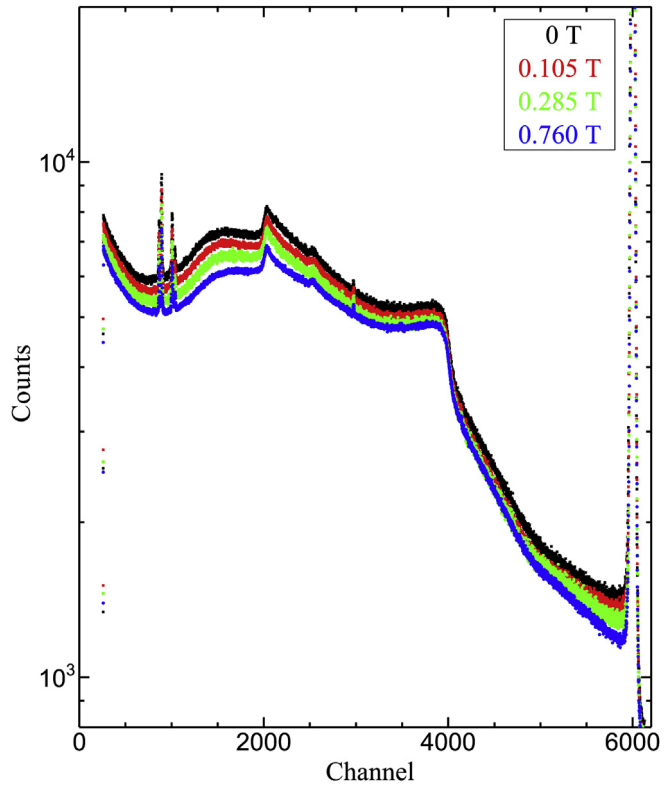

Fig. 8. The DB spectra measured in a magnetic field of 0, 0.105, 0.285, and 0.760 T. The maximum count of 511 keV peak (~ 6000 channel) was normalized to 1×10^5 for each spectrum. The channel width is 85.57 eV/channel. (For interpretation of the references to colour in this figure legend, the reader is referred to the Web version of this article.)

$$I_{|+\rangle}^{3\gamma} = \left(1 - R_{\text{pick-off}}^{2\gamma} \frac{\tau_{|+\rangle}}{\tau_{\text{o-Ps}}}\right) \frac{\lambda_{\text{o-Ps}}}{\lambda_{\text{o-Ps}} + y^2 \lambda_{\text{p-Ps}}} I_{|+\rangle}, \tag{28}$$

$$I_{|-\rangle}^{3\gamma} = \frac{y^2 \lambda_{\text{o-Ps}}}{\lambda_{\text{p-Ps}} + y^2 \lambda_{\text{o-Ps}}} I_{|-\rangle}. \tag{29}$$

In Fig. 9, we show the intensities of the 3γ decay of Ps atoms in the four states with magnetic field increasing up to 0.760 T: (a) $I_{|1,1\rangle}^{3\gamma}$ and (b) $I_{|1,-1\rangle}^{3\gamma}$ keep as a constant of 8.07%, (c) $I_{|+\rangle}^{3\gamma}$ decreases drastically from 8.07% to 0.94%, (d) $I_{|-\rangle}^{3\gamma}$ increases from 0 to only 0.012% and thereafter could be neglected. In general, the variation of $I_{\text{Ps}}^{3\gamma}$ of all Ps atoms shows the same tendency with that of $I_{|+\rangle}^{3\gamma}$.

To study the intensity of low energy region (below 511 keV peak) which is correlated with the fraction of 3γ decay of Ps ($F_{\text{Ps}}^{3\gamma}$), a function R is defined as (Lynn and Welch, 1980; Kawasuso et al., 2013; Zhang et al., 2014):

$$R = \frac{T - U}{U} = \frac{(1 - F_{Ps}^{3\gamma})R_0 + F_{Ps}^{3\gamma} R_1 U_1 / U_0}{1 - F_{Ps}^{3\gamma} + F_{Ps}^{3\gamma} U_1 / U_0}, \tag{30}$$

where T is the total area under the intensity curve, U is the area under the 511 keV peak, and the subscripts 0 and 1 of R and U denote 0% and 100% Ps formation, respectively. For a small o-Ps formation fraction ($F_{Ps}^{3\gamma}$), $\Delta R = R - R_0 \propto F_{Ps}^{3\gamma}$. For the measurement of R_0 (no Ps formed in a sample if high energy positrons are injected into a vacancy-free sample) and R_1 (100% Ps could be formed on the surface of a single-crystal (vacancy-free) metal by injecting low energy (a few tens of eV) positrons to the sample), a slow positron beam and a vacancy-free sample are needed (Lynn and Lutz, 1980). In this study, the γ-Al_2O_3 sample contains a large number of free volumes that quite suitable for Ps formation. So R_0 could not be realized even with the high energy positrons from a slow positron beam, therefore it is impossible to quantitatively

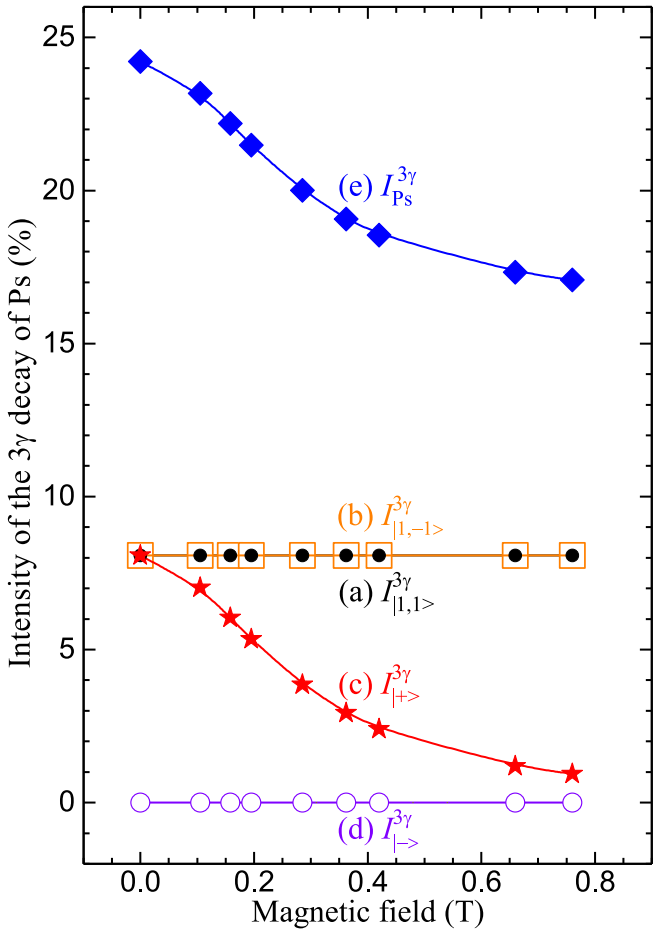

Fig. 9. The intensity of 3γ decay of Ps for (a) $|1,1\rangle$ state ($I_{|1,1\rangle}^{3\gamma}$), (b) $|1,-1\rangle$ state ($I_{|1,-1\rangle}^{3\gamma}$), (c) $|+\rangle$ state ($I_{|+\rangle}^{3\gamma}$.), (d) $|-\rangle$ state ($I_{|-\rangle}^{3\gamma}$), (e) all Ps states ($I_{\text{Ps}}^{3\gamma}$, the sum of (a), (b), (c), and (d), derived from magnetic quenching theory), as a function of magnetic field. (For interpretation of the references to colour in this figure legend, the reader is referred to the Web version of this article.)

determine the $F_{Ps}^{3\gamma}$ and $I_{Ps}^{3\gamma}$ of γ-Al_2O_3 nanopowder by DB measurements.

In this study, to calculate the value of R, the range between 0 to 6050 channel is selected for the T, and the range between 5950 to 6050 channel is selected for the U. The variation of R as a function of magnetic field is plotted in Fig. 10. The tendency of R is clear, it first decreases quickly for the magnetic field less than 0.420 T, and then decreases much slowly after the magnetic field exceeds 0.420 T. While in Fig. 9, we could find more or less similar tendency for $I_{|+\rangle}^{3\gamma}$ and $I_{\text{Ps}}^{3\gamma}$. This proves that R (ratio between the area of the low energy region and the area of 511 keV peak region) reflects the 3γ decay of Ps atoms.

5. Conclusions

In the present work, we experimentally studied the magnetic quenching of Ps atoms in a series of static magnetic fields by PAL and DB measurements in γ-Al_2O_3 nanopowder. We could conclude the magnetic quenching of Ps atoms in γ-Al_2O_3 nanopowder in five aspects: (1) The mean lifetime of long-lived Ps atoms is quenched by magnetic field due to the short lifetime of $|+\rangle$ state; (2) The formation probability of each Ps state is not affected by magnetic field; (3) The intensity of the narrow component of DB spectrum is increased by 2γ decay of $|+\rangle$ state; (4) The FWHM of the narrow component of DB spectrum is narrowed by the 2γ decay of $|+\rangle$ state; (5) The intensity of the low energy region of DB spectrum is diminished by the decrease of 3γ decay of $|+\rangle$ state. These experimental results enable us to study some complex quenching effects of Ps which are mixed from magnetic

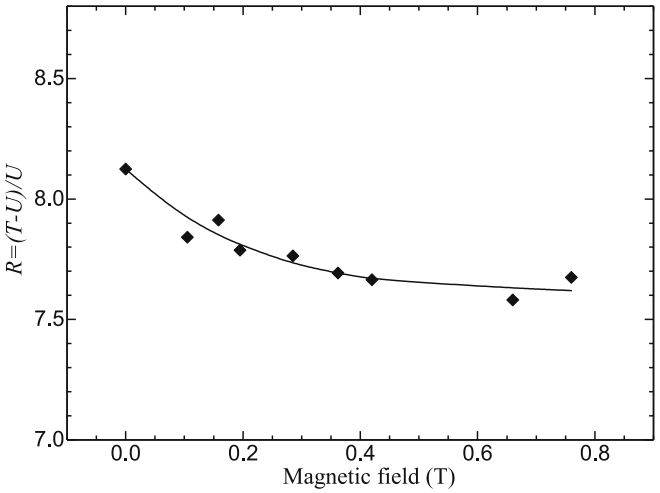

Fig. 10. Variation of $R = (T - U)/U$ of the DB spectra as a function of magnetic field.

quenching and some other effects.

Acknowledgements

This work was financially supported by the National Natural Science Foundation of China under Grant Nos. 11975225, 11875248, and 11775215.

References

Bisi, A., Fiorentini, A., Gatti, E., Zappa, L., 1962. Magnetic quenching of positronium in solids and positron helicity. Phys. Rev. 128 (5), 2195.
Brandt, W., Paulin, R., 1968. Positronium diffusion in solids. Phys. Rev. Lett. 21 (4), 193.
Chen, Z.Q., Ma, L., Wang, S.J., 1995. Study of the surface properties zeolite using positron annihilation technique. Phys. Status Solidi 147 (1), 187–193.
Chen, Z.Q., Maekawa, M., Yamamoto, S., Kawasuso, A., Yuan, X.L., Sekiguchi, T., Suzuki, R., Ohdaira, T., 2004. Evolution of voids in Al^+-implanted ZnO probed by a slow positron beam. Phys. Rev. B 69 (3), 035210.
Chen, Z.Q., Kawasuso, A., Xu, Y., Naramoto, H., Yuan, X.L., Sekiguchi, T., Suzuki, R., Ohdaira, T., 2005. Microvoid formation in hydrogen-implanted ZnO probed by a slow positron beam. Phys. Rev. B 71 (11), 115213.
Chuang, S.Y., Tao, S.J., 1970. Study of inhibition and quenching of positronium by iodine and CCl_4. J. Chem. Phys. 52 (2), 749–751.
Coleman, P., 2000. Positron Beams and Their Applications. World Scientific, Singapore.
Consolati, G., 1996. Magnetic quenching of positronium. J. Radioanal. Nucl. Chem. 210 (2), 273–292.
Deng, Q., Jean, Y.C., 1993. Free-volume distributions of an epoxy polymer probed by positron annihilation: pressure dependence. Macromolecules 26 (1), 30–34.
Deutsch, M., 1951. Evidence for the formation of positronium in gases. Phys. Rev. 82 (3), 455.
Deutsch, M., Brown, S.C., 1952. Zeeman effect and hyperfine splitting of positronium. Phys. Rev. 85 (6), 1047.
Deutsch, M., Dulit, E., 1951. Short range interaction of electrons and fine structure of positronium. Phys. Rev. 84 (3), 601.
Halpern, O., 1954. Magnetic quenching of the positronium decay. Phys. Rev. 94 (4), 904.
Hyodo, T., Nakayama, T., Saito, H., Saito, F., Wada, K., 2009. The quenching of ortho-positronium. Phys. Status Solidi 6 (11), 2497–2502.
Ito, K., Nakanishi, H., Ujihira, Y., 1999. Extension of the equation for the annihilation lifetime of ortho-positronium at a cavity larger than 1 nm in radius. J. Phys. Chem. B 103 (21), 4555–4558.
Itoh, Y., Murakami, H., Kinoshita, A., 1993. Positron annihilation in porous silicon. Appl. Phys. Lett. 63 (20), 2798–2799.
Kawasuso, A., Fukaya, Y., Maekawa, M., Zhang, H.J., Seki, T., Yoshino, T., Saitoh, E., Takanashi, K., 2013. Current-induced spin polarization on a Pt surface: a new approach using spin-polarized positron annihilation spectroscopy. J. Magn. Magn. Mater. 342, 139–143.
Kirkegaard, P., Pedersen, N.J., Eldrup, M.M., 1989. PATFIT-88: A Data-Processing System for Positron Annihilation Spectra on Mainframe and Personal Computers. Risø National Laboratory, Grafisk Service, Risø, Denmark.
Liu, Z.W., Zhang, H.J., Chen, Z.Q., 2014. Monolayer dispersion of CoO on Al_2O_3 probed by positronium atom. Appl. Surf. Sci. 293, 326–331.
Lue, S.J., Lee, D.T., Chen, J.Y., Chiu, C.H., Hu, C.C., Jean, Y.C., Lai, J.Y., 2008. Diffusivity enhancement of water vapor in poly (vinyl alcohol)–fumed silica nano-composite membranes: correlation with polymer crystallinity and free-volume properties. J. Membr. Sci. 325 (2), 831–839.
Lynn, K.G., Lutz, H., 1980. Slow positrons in single-crystal samples of Al and Al-Al_xO_y. Phys. Rev. B 22 (9), 4143.
Lynn, K.G., Welch, D.O., 1980. Slow positrons in metal single crystals. I. positronium formation at Ag(100), Ag(111), and Cu(111) surfaces. Phys. Rev. B 22 (1), 99.
Mills Jr., A.P., 1975. Effects of collisions on the magnetic quenching of positronium. J. Chem. Phys. 62 (7), 2646–2659.
Mitroy, J., Novikov, S.A., 2003. Spin-orbit quenching of positronium during atomic collisions. Phys. Rev. Lett. 90 (18), 183202.
Mohorovic, V.S., 1934. Möglichkeit neuer elemente und ihre bedeutung für die astrophysik. Astron. Nachr. 253 (4), 93.
Nagashima, Y., Kakimoto, M., Hyodo, T., Fujiwara, K., Ichimura, A., Chang, T., Deng, J., Akahane, T., Chiba, T., Suzuki, K., et al., 1995. Thermalization of free positronium atoms by collisions with silica-powder grains, aerogel grains, and gas molecules. Phys. Rev. A 52 (1), 258.
Paulin, R., Ambrosino, G., 1968. Annihilation libre de l'ortho-positonium formé dans certaines poudres de grande surface spécifique. J. Phys. 29 (4), 263–270.
Rich, A., 1981. Recent experimental advances in positronium research. Rev. Mod. Phys. 53 (1), 127.
Rochanakij, S., Schrader, D.M., 1988. Magnetic quenching of positronium in organic solutions. Radiat. Phys. Chem. 32 (3), 557–561.
Saito, H., Hyodo, T., 1999. Quenching of positronium by surface paramagnetic centers in ultraviolet-and positron-irradiated fine oxide grains. Phys. Rev. B 60 (15), 11070.
Saito, H., Hyodo, T., 2006. Experimental evidence for spin-orbit interactions in positronium-Xe collisions. Phys. Rev. Lett. 97 (25), 253402.
Sato, K., Ito, K., Hirata, K., Yu, R.S., Kobayashi, Y., 2005. Intrinsic momentum distributions of positron and positronium annihilation in polymers. Phys. Rev. B 71 (1), 012201.
Schrader, D.M., Jean, Y.C., 1988. Positron and Positronium Chemistry. Elsevier.
Shibuya, K., Nakayama, T., Saito, H., Hyodo, T., 2013. Spin conversion and pick-off annihilation of ortho-positronium in gaseous xenon at elevated temperatures. Phys. Rev. A 88 (1), 012511.
Shinohara, N., Suzuki, N., Chang, T., Hyodo, T., 2001. Pickoff and spin conversion of orthopositronium in oxygen. Phys. Rev. A 64 (4), 042702.
Skalsey, M., Engbrecht, J.J., Bithell, R.K., Vallery, R.S., Gidley, D.W., 1998. Thermalization of positronium in gases. Phys. Rev. Lett. 80 (17), 3727.
Tao, S.J., 1970. Positronium and iodine reactions in organic solvents. J. Chem. Phys. 52 (2), 752–757.
Tao, S.J., 1972. Positronium annihilation in molecular substances. J. Chem. Phys. 56 (11), 5499–5510.
Trueba, M., Trasatti, S.P., 2005. γ-alumina as a support for catalysts: a review of fundamental aspects. Eur. J. Inorg. Chem. 2005 (17), 3393–3403.
Zhang, H.J., Wang, D., Chen, Z.Q., Wang, S.J., Xu, Y.M., Luo, X.H., 2008. Positron annihilation study of Mo dispersion in MoO_3/Al_2O_3 catalysts. Acta Phys. Sin. 57 (11), 7333.
Zhang, H.J., Chen, Z.Q., Wang, S.J., Kawasuso, A., Morishita, N., 2010. Spin conversion of positronium in NiO/Al_2O_3 catalysts observed by coincidence Doppler broadening technique. Phys. Rev. B 82 (3), 035439.
Zhang, H.J., Liu, Z.W., Chen, Z.Q., Wang, S.J., 2011. Chemical quenching of positronium in CuO/Al_2O_3 catalysts. Chin. Phys. Lett. 28 (1), 017802.
Zhang, H.J., Chen, Z.Q., Wang, S.J., 2012. Monolayer dispersion of NiO in NiO/Al_2O_3 catalysts probed by positronium atom. J. Chem. Phys. 136 (3), 034701.
Zhang, H.J., Yamamoto, S., Fukaya, Y., Maekawa, M., Li, H., Kawasuso, A., Seki, T., Saitoh, E., Takanashi, K., 2014. Current-induced spin polarization on metal surfaces probed by spin-polarized positron beam. Sci. Rep. 4, 4844.